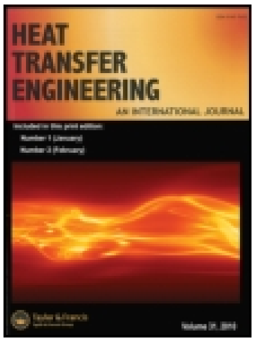

Heat Transfer Engineering

ISSN: 0145-7632 (Print) 1521-0537 (Online) Journal homepage: https://www.tandfonline.com/loi/uhte20

Heat Transfer and Fluid Flow on Dimpled Surface With Bleed Flow

Heeyoon Chung , Kyung Min Kim , Hyun Goo Kwon , Sanghoon Lee , Beom Seok Kim & Hyung Hee Cho

To cite this article: Heeyoon Chung , Kyung Min Kim , Hyun Goo Kwon , Sanghoon Lee , Beom Seok Kim & Hyung Hee Cho (2014) Heat Transfer and Fluid Flow on Dimpled Surface With Bleed Flow, Heat Transfer Engineering, 35:6-8, 641-650, DOI: 10.1080/01457632.2013.837695

To link to this article: https://doi.org/10.1080/01457632.2013.837695

Heat Transfer Engineering, 35(6–8):641–650, 2014

ISSN: 0145-7632 print / 1521-0537 online
DOI: 10.1080/01457632.2013.837695

Heat Transfer and Fluid Flow on Dimpled Surface With Bleed Flow

HEEYOON CHUNG, KYUNG MIN KIM, HYUN GOO KWON, SANGHOON LEE, BEOM SEOK KIM, and HYUNG HEE CHO

Department of Mechanical Engineering, Yonsei University, Seoul, Korea

This study investigates the effects of bleed flow on heat transfer and fluid flow on a dimpled surface in a rectangular channel. The heat transfer on a dimpled surface with bleed flow is compared with that on a dimpled surface without bleed flow. The height of the channel is 15.0 mm. The dimples are arrayed in staggered on the bottom surface of the channel with a pitch of 15.0 mm. The dimple depth is 3.75 mm and the dimple footprint diameter is 13.0 mm. The bleed hole is installed on the inner surface of the dimple and the diameter of the hole is 1.3 mm. The tests were conducted with varying Reynolds numbers from 1000 to 10,000 and 0.5% of total mass flow is flowing out through a bleed hole. A numerical method was employed to determine the detailed heat transfer coefficients. Commercial computational fluid dynamics software, ANSYS CFX 13.0, is adopted and the Shear Stress Transport model is set to turbulent model. As a result, the overall heat transfer rate on dimpled surface with bleed flow is 10–20% higher than that without bleed flow.

INTRODUCTION

The gas turbine is now a widely used power-generating system due to its wide capacity, from kilo- to megawatts, and reliable performance. Like other thermal power systems, its efficiency is directly proportional to operating temperature, which is specifically called the turbine inlet temperature. Therefore, a lot of efforts were made to increase the turbine inlet temperature, and major components of the gas turbine, such as combustor and turbine blades, are exposed to extremely hot combustion gas. But there is a limitation in raising the turbine inlet temperature because of the maximum allowable temperature of the material. Also, continuous thermal stress is the most frequent cause in failure of gas turbine engines and it also significantly affects their life span. To increase the efficiency and life span of gas turbine engine, designing an effective cooling system has become a prerequisite process in development of high-performance gas turbine engines. The incipient idea of this cooling technique is to make an internal passage inside the components and let cooling fluid flow. This is now avery common technique, and various advanced internal cooling passages are implemented to improve gas turbine performance.

In an internal cooling passage, the characteristic of heat transfer is mainly dominated by turbulent transport and secondary flow, which is induced by geometrical features. This means that better cooling performance could be obtained by adding or modifying geometries of the internal passage. Special geometries, such as ribs, fins, protrusion, and dimple, have been investigated as a heat transfer intensifier. Especially the dimple, a spherically concave structure on the surface, has advantages over others in aspects of heat transfer and pressure drop [1]. Many studies were conducted about the characteristics of heat transfer and flow fields on a dimpled surface. Chyu et al. [2] investigate the effect of dimples in a rectangular channel using a transient liquid crystal method. Their result shows that dimples enhanced heat transfer level by about 2.5 times. Mahmood et al. [3] experimentally identified vortical fluid flow and vortex shedding downstream of the dimple. Moreover, they verified that these vortices enhance the heat transfer rate of the dimple. Burgress et al. [4] presented a detailed explanation of the flow structure and heat transfer in a channel with dimple arrays. They provided flow visualization of an instantaneous flow structure induced within a dimple. The globally averaged Nusselt number in their results increased with the dimple depth, and the heat transfer augmentation factors ranged from 1.5 to 2.5 as the dimple depth increased. Hwang et al. [5, 6] compared an array of dimple and protrusion in rectangular channels through the experimental method of transient

The authors gratefully acknowledge that this work is supported by the Korea Government Ministry of Knowledge Economy. This work was supported by the aerospace research program (KA00157) of Korea Aerospace Research Institute (KARI) and the human resources development program (No. 20134030200200) of the Korean Institute of Energy Technology Evaluation and Planning (KETEP). Those programs are funded by the Korean government Ministry of Trade, Industry and Energy.

Address correspondence to Professor Hyung Hee Cho, Yonsei University, Sinchon-dong, Seodaemun-gu, Seoul, Republic of Korea. E-mail: hhcho@yonsei.ac.kr

liquid crystals (TLC). Enhanced heat transfer rate with relatively low friction factor was applied in a channel with a dimpled surface. Kwon [7] and Kwon et al. [8] investigated local heat and mass transfer on a single dimple with varying dimple depth using a naphthalene sublimation method. They indicated that heat and mass transfer and secondary flow are strengthened as dimple depth and Reynolds number are increased. Isaev and Leont'ev [9] performed a numerical simulation of a vortex flow and heat transfer in the vicinity of a dimple using the Reynolds averaged Navier–Stokes (RANS) method. They analyzed a tornado-like mechanism for enhancing the heat transfer in a spherical dimple with varying depth under conditions of turbulent flow. Most of the preceding studies reported that there exists recirculating flow, which is trapped inside the dimple, and it aggravates the heat transfer performance of the dimple.

A film cooling method has been employed as a further advanced cooling technique for gas turbine components besides augmentation of heat transfer in internal passage. Internal cooling fluid is ejected through the holes on the surface of components and then a thin film of cooling flow is formed on the surface to protect the outer surface of components that are directly exposed to hot gas. To perform a film cooling, bleed holes are placed in an internal cooling passage, and internal cooling performance is affected because cooling fluid is flowing from them. There are earlier studies about the effect of bleed flow in an internal passage. Kim et al. [10] performed an experiment comparing the effect of bleed flow on heat transfer performance in a channel. The results show that bleed flow improved overall heat transfer performance as the flow rate increased. Taslim et al. [11] measured local heat transfer coefficients in trapezoidal passages with bleed holes, and reported that bleed holes on the smooth surface consequently yield a more uniform distribution of span-wise heat transfer coefficient on the ribbed surface and the bleed flow caused lower friction factor than in the case of no effusion. Shen et al. [12] studied heat transfer enhancement by ribs and the combination of ribs and bleed holes. They found that the average heat transfer in the latter case was approximately 25% higher than that in the former case, but the heat transfer was decreased at high bleed ratios. Thurman and Poinsatte [13] investigated the interaction of 90-degree ribs and various bleed conditions on heat transfer. They reported that placing bleed holes after ribs widened the regions of high heat transfer due to removing the recirculation flow behind the ribs. A similar result was reported by Jeon et al. [14] within the rotating channel.

The main idea of this research is to compensate heat transfer performance of dimpled surface with bleed flow. It was proven through earlier studies that large recirculating flow exists inside the dimple, which deteriorates heat transfer performance. In making a bleed hole inside the dimple cavity to let cooling fluid flow out through it, the heat transfer rate would be increased as much as the total flow rate of cooling fluid into the dimple is increased. Additionally, we could expect to diminish the size of recirculating flow. A conceptual schematic of present study is given in Figure 1. There are already a lot of studies for dimple cavity and bleed flow for film cooling as separated subjects.

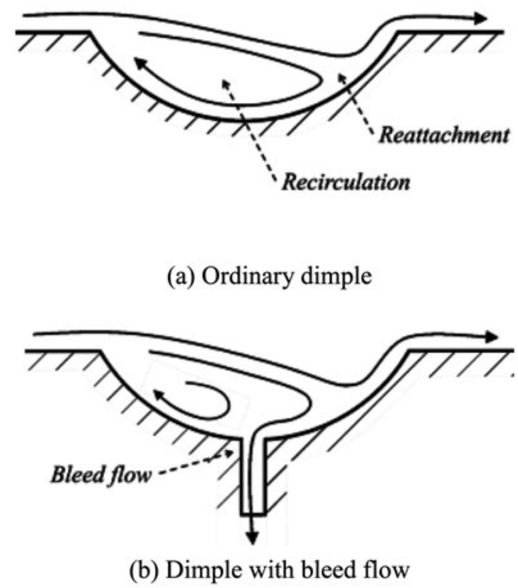

Figure 1 Conceptual scheme of present study.

However, few attempts were made to combine these two methods. In this research, the synergy effect of dimple cavity and bleed flow would be verified using a numerical method.

TEST SETUP AND NUMERICAL METHOD

As shown in Figures 2b and 2c, two test domains are presented to compare the effect of bleed flow on dimpled surface. Flow in the box that is indicated with the dashed line is assumed to be fully developed. Therefore, all figures and data were taken from this area. Dimples are arrayed with a staggered pattern on the bottom surface of rectangular channel. Bleed holes are placed at the bottom of the dimple cavities in Figure 2c, and 0.5% of total mass flow is flowing out through each bleed hole. This flow rate is calculated based on the ratio of the area of channel to the size of bleed hole. The specific dimension of the channel and single dimple were determined based on experimental study done by Hwang et al. [5] as presented in Figure 2.

The height of the channel *(H)* is 15 mm and the width *(W)* is 15 mm. The total length (L_1) is 190 mm and it contains 12 rows of dimples and its pitch *(P)* is 15 mm. A translational periodic condition is imposed on the span-wise direction of the channel. Then it can be regarded as a wide duct. The hydraulic diameter (D_h) of the channel is set to 26.25 mm, which comes from the experimental setup of Hwang et al. [5]. The print diameter of the dimple *(d)* is 13 mm and the dimple depth *(h)* is 3.75 mm ($h/H = 0.25$). A constant mass flow rate is imposed on both inlet and outlet.

Tests were conducted with varying Reynolds number, from 1,000 to 10,000. The Reynolds number is defined as follows:

$$\mathrm{Re}_{Dh} = \frac{UD_h}{v} \quad (1)$$

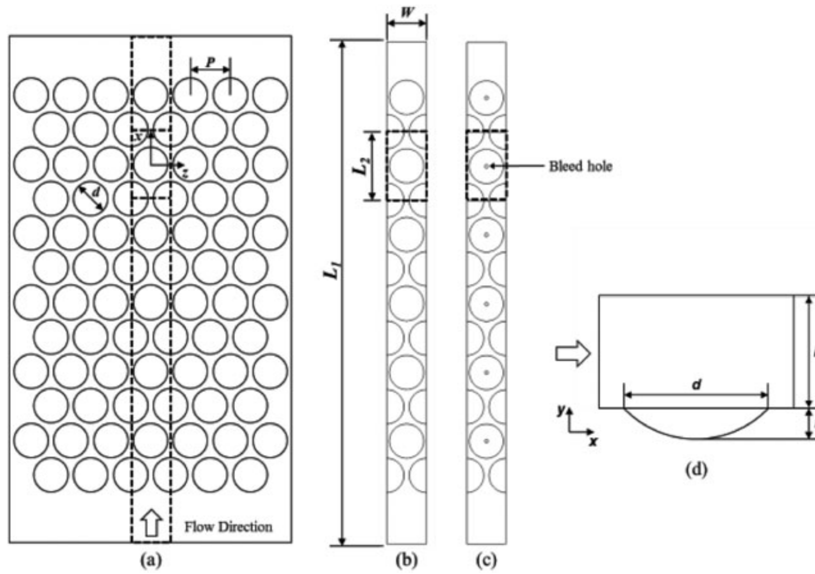

Figure 2 Geometries: (a) experimental test section of Hwang et al. [5]; (b) flow domain without bleed flow; (c) flow domain with bleed flow; (d) specific dimensions of the dimple and channel.

where U is average velocity at the inlet, which varies to adjust to the Reynolds number. Kinematic viscosity, v, is assumed to be a constant value equal to 18.31×10^{-6} m^2/s.

The bottom surface of the channel is heated with a constant-temperature condition, $T_w = 330$ K, and the top surface is set to be an adiabatic wall. Cooling air at 300 K is flowing from the entrance of channel. The dimensionless heat transfer coefficient, the Nusselt number, is calculated as follows:

$$\mathrm{Nu} = \frac{hD_h}{k_{air}} \tag{2}$$

where the heat transfer coefficient, h, is calculated based on an average temperature inside the box with dashed line which is designated in Figure 2. Air is regarded as an ideal gas with a constant thermal conductivity, $k = 0.0261$ W/m-K.

The area-averaged Nusselt number is calculated as in the following integration:

$$\overline{\overline{\mathrm{Nu}}} = \frac{\int_{x/d=-1}^{x/d=1} \int_{z/d=0.5}^{z/d=0.5} \mathrm{Nu} dz dx}{A} \tag{3}$$

As mentioned earlier, the Nusselt number is averaged over the area bounded with the dashed line as illustrated in Figures 2a and 2b.

The friction factor, f, is defined as follows:

$$f = \frac{1}{2} \Delta P \frac{D_h}{L_2 \rho_{air} U^2} \tag{4}$$

where ΔP is pressure loss, while the flow is across the channel length L, U is the average velocity at the channel inlet, and ρ_{air} is density of air.

The performance factor, PF, is considering both the heat transfer augmentation and the pressure loss. The performance factor is defined as

$$\mathrm{PF} = \frac{\mathrm{Nu}/\mathrm{Nu}_0}{(f/f_0)^{1/3}} \tag{5}$$

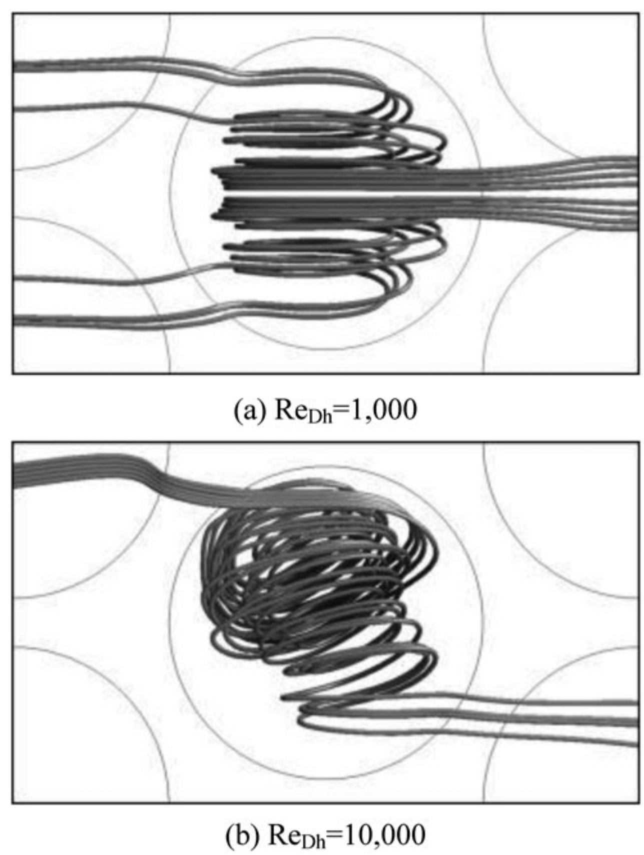

Figure 3 Different dominant flow structures inside the dimple in laminar flow regime and in turbulent flow regime.

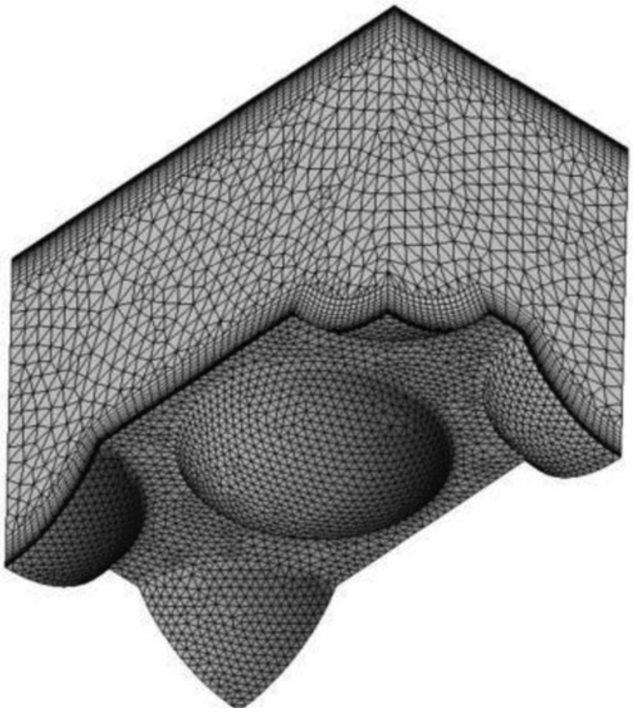

Figure 4 Grid resolution.

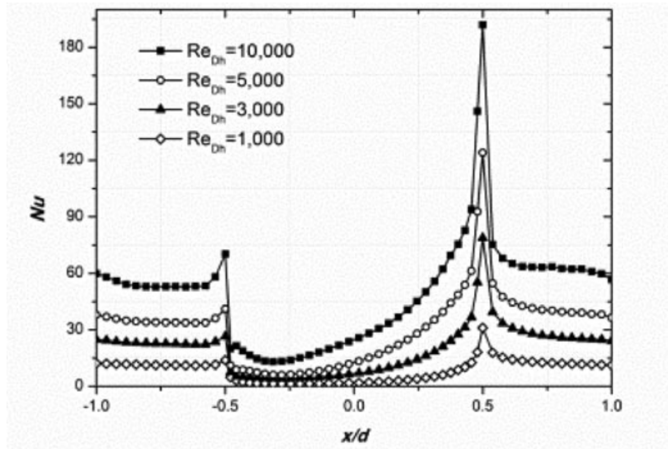

(a) Result of present study

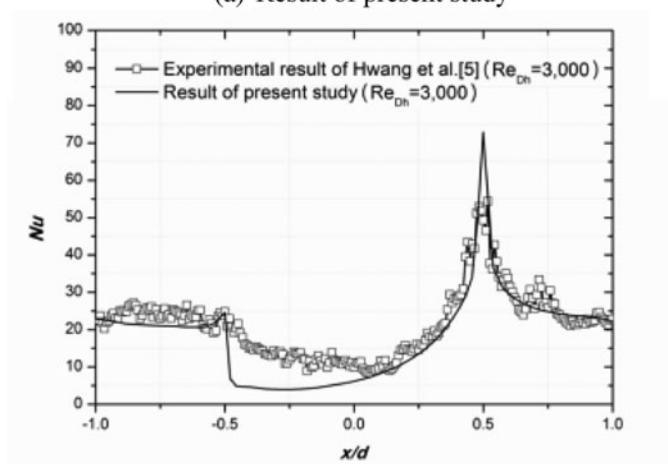

(b) Comparison with experimental result of Hwang et al.[5]

Figure 5 Distribution of Nusselt number along stream wise direction ($z/d = 0$).

where Nu_0 and f_0 are the averaged Nusselt number and the friction factor of the smooth channel, respectively. The Nusselt number and the friction factor for the smooth channel were also calculated using identical operating conditions.

All calculations are performed with commercial computational fluid dynamics (CFD) software, ANSYS CFX 13.0. Reynolds averaged Navier–Stokes (RANS) equation is solved for the steady state problem. A zonal k-w model, Shear Stress Transport (SST), was adopted for a turbulent model for this simulation because Isaev and Leont'ev [9] successfully depicted the vortex structure on dimpled surface by using this model. They reported that a symmetric vortex is observed in the laminar flow regime and an asymmetric vortex is observed in the turbulent flow regime. Figure 3 is a graphical representation of these two distinctive vortices clearly captured by the present study. Grids are generated with about 1,100,000 elements. Fifteen prism layers are accumulated on the boundary layer with very fine resolution to capture the separation and the reattachment of flow adjacent to the dimpled surface and the y+ value is less than 1 in all cases. The free stream region is filled with tetrahedrons. Figure 4 shows the grid resolution of flow domain.

RESULT AND DISCUSSION

In general, the flow structure on dimpled surface can be explained by flow separation, flow reattachment, secondary flow induced by flow, and geometric condition. The main flow separates at the upstream edge of the dimple, and then the separated flow impinges around the rear rim of the dimple. After the impingement, the flow is divided into a symmetric dual vortex in the dimple cavity. This dual vortex occupies almost of all volume of the cavity and circulates along the curvature with relatively low velocity. Main flow cannot reach the bottom of the dimple cavity due to this recirculating flow. Instead, it flows over the dimple, generating a median vortex. This vortex develops the mixing layer above the recirculating region and a small portion of recirculating flow is mixed with the median vortex in the mixing layer. If the Reynolds number is increased up to a turbulent flow regime, the flow around the dimple is distorted. The symmetric dual vortex turns to a tornado-like asymmetric vortex and the median vortex is biased along with the asymmetric vortex. In addition, self-oscillating unsteadiness is observed. Extension of the mixing layer induces more external flow infiltrating into the dimple cavity. This phenomenon is explained in detail by Gortyshov and Popov [15] and reproduced in the present study.

Heat Transfer Characteristics

Distribution of the Nusselt number along the stream wise direction is plotted at $z/d = 0$ in Figure 5. The result of present

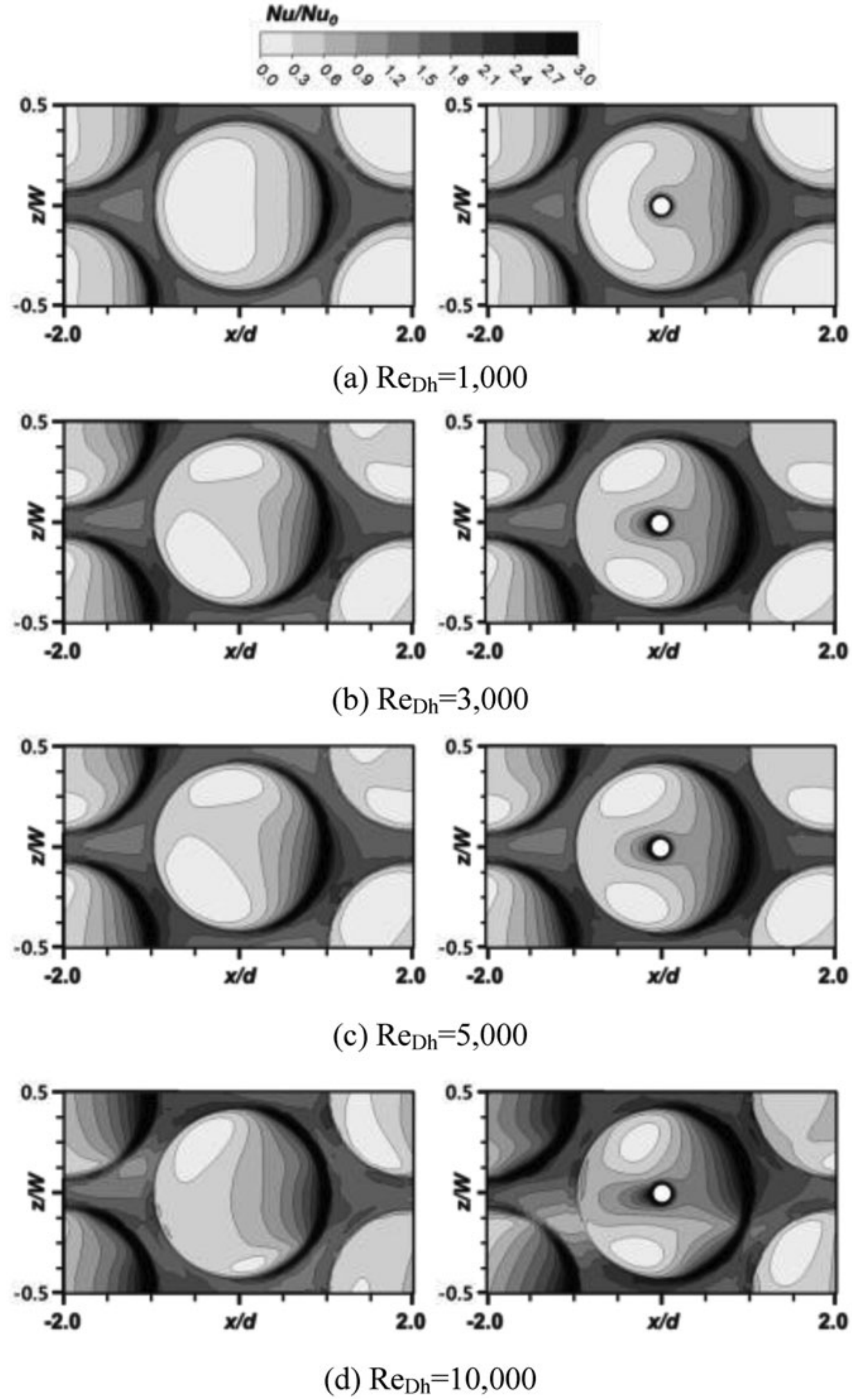

Figure 6 Contours of normalized Nusselt number at the bottom surface with varying Reynolds number.

study is compared with the experimental result of Hwang et al. [5]. The stream direction is from left to right. The experimental and the numerical results look quite similar. The lowest Nusselt number appears near the front region inside the dimple as soon as flow is separated from the surface. Then Nusselt number is ascending while flow is moving downstream of the dimple surface. The peak Nusselt number appears near the rear rim of each dimple where the separated flow reattaches. However, quantitative differences are present. The Nusselt numbers of numerical result shows relatively lower values than the experimental result. A similar result was reported by Park et al. [16]. They conducted numerical simulation of heat transfer on the dimpled channel using the Reynolds averaged Navier–Stokes (RANS) method. Even though the RANS method underestimated heat transfer

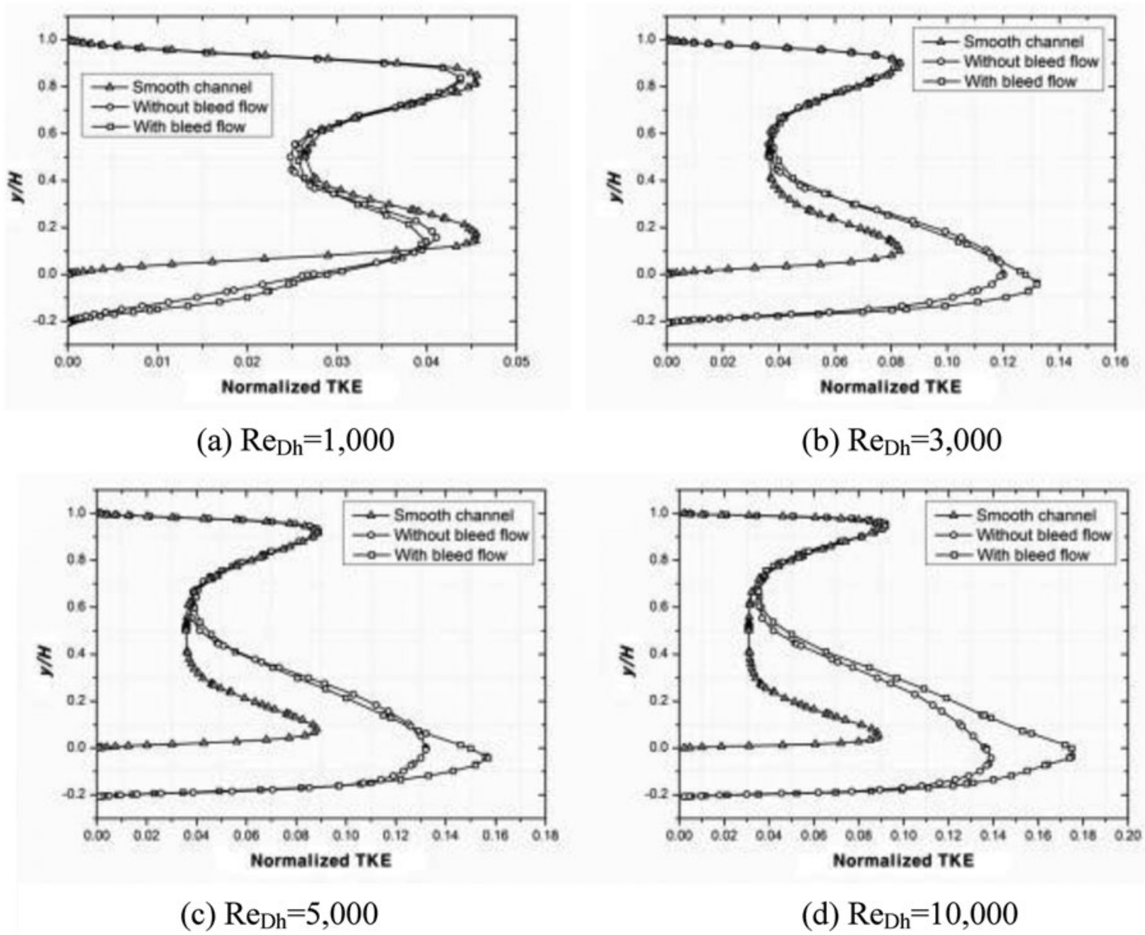

Figure 7 Distributions of normalized turbulence kinetic energy at $x/d = 0.25$ and $z/d = 0$.

on the dimpled channel, important features of flow above the dimple are properly captured.

The contours of the normalized Nusselt number in all cases are presented in Figure 6; the left ones are the result of the dimple without bleed flow cases and the right ones are from the dimple with bleed flow cases. The contours of normalized Nusselt number correspond to the flow structure above the dimple as explained earlier. In the laminar flow regime (Re_{Dh} = 1,000), a relatively high heat transfer rate is presented on the rear rim of the dimple as separated upstream flow impinges. But if the amount of upstream penetrating flow into the dimple cavity is relatively small then overall heat transfer rate deteriorates because the recirculation dominates all over the surface on the cavity. When the recirculation occurs, fluid moves at a relatively low velocity and is trapped in the cavity for a while. Then heat energy inside the cavity cannot disperse outward. This phenomenon is different in the turbulent flow regime ($3000 \leq Re_{Dh}$). The amount of upstream flow penetrating into the dimple cavity increases as the Reynolds numbers increases. Since the nature of turbulent flow is asymmetric and self-oscillating, it enhances mixing between upstream and recirculating flow in the dimple cavity. The heat transfer rate on the rear rim of the dimple is conspicuously augmented. In addition, the main stream flowing over the dimple is pulled down to the surface of channel by the enhanced mixing effect and then more upstream flow impinges on the rear rim of the dimple. Highly enhanced heat transfer appears on the downstream surface right behind the dimple cavity. Overall heat transfer performance is improved on dimpled surface.

In all cases of dimple with bleed flow, heat transfer rate is locally magnified in the vicinity of the bleed hole since fluid is accelerated while flowing out through it. The impinging region on rear rim is drawn down because relatively low pressure presents in the vicinity of bleed holes. The benefit of bleed flow is more remarkable in a turbulent flow regime. As flow structure becomes asymmetric, heat transfer rate is irregularly distributed and highly enhanced heat transfer regions are clearly observed at downstream of the dimple. It looks much more intense than that in the case of without bleed flow.

To explain more details about heat transfer enhancement mechanism for dimple, the normalized turbulent kinetic energy is plotted along the y-direction with the rear side of the dimple ($x/d = 0.25$ and $z/d = 0$) in Figure 7. Turbulence is a good transport mechanism for heat energy and momentum of fluid, and it

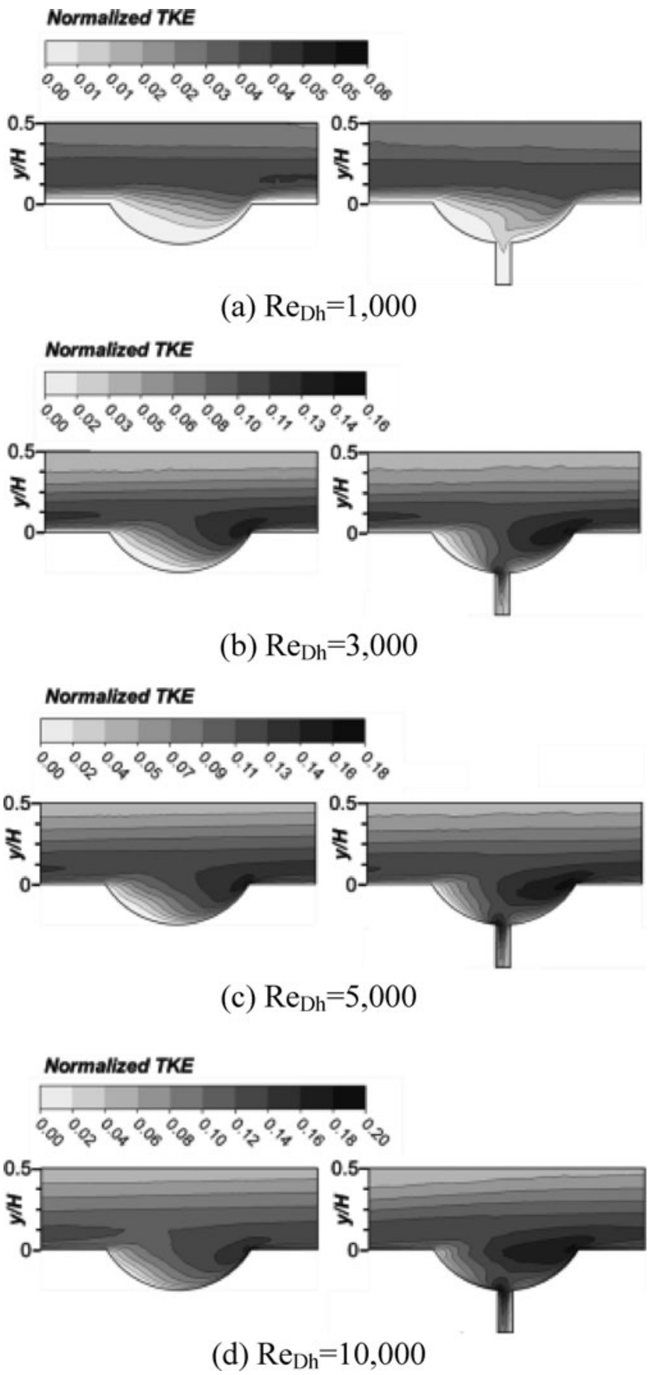

Figure 8 Contours of normalized turbulence kinetic energy at the mid-plane of channel along stream wise direction ($z/d = 0$).

is represented by turbulent kinetic energy, which is kinetic energy of the fluctuating velocity of the fluid. The turbulent kinetic energy is presented being normalized by the square of the free stream velocity in the present study. In the laminar flow regime ($Re_{Dh} = 1{,}000$), there are no big differences in turbulent kinetic energy level between the two cases. The maximum turbulent kinetic energy is even lower than that of the smooth surface. The momentum of laminar flow is not enough to generate disturbance at the downstream region of dimple, and it causes the dimple to show lower heat transfer performance than that of the smooth channel. On the other hand, turbulent kinetic energy around the rear rim of the dimple is significantly increased in the turbulent flow regime ($3000 \leq Re_{Dh}$). This accounts for how heat transfer rate is enhanced downstream of the dimple in the high Reynolds number flow. In all cases of dimple with bleed flow, the maximum turbulent kinetic energy is higher than that of without bleed flow cases. The amount of difference of maximum level is enlarged as the Reynolds number is increasing.

In Figure 8, contours of the normalized turbulent kinetic energy on the mid-plane of the channel where $z/d = 0$ are presented. The heat transfer enhancement mechanism for the dimple with bleed flow case is more comprehensive with these figures. As explained earlier with Figure 7, the turbulent kinetic energy around the rear region of the dimple is highly intensive except in the laminar flow case ($Re_{Dh} = 1000$). Comparing results of in the case of dimple with bleed flow and without bleed flow, the region of highly enhanced turbulent kinetic energy is fairly widened with bleed flow. As bleed flow draws down the flow to the surface, more fluid thus impinges to the rear rim of the dimple and it results in enhancing heat transfer rate downstream of the dimple. Additionally, the turbulent kinetic energy around the bleed hole is increased as recirculating flow inside the dimple, which moves at relatively low velocity, is flowing out through the bleed hole, accelerating its speed. The consequent turbulent kinetic energy profile shows good correspondence with the heat transfer result.

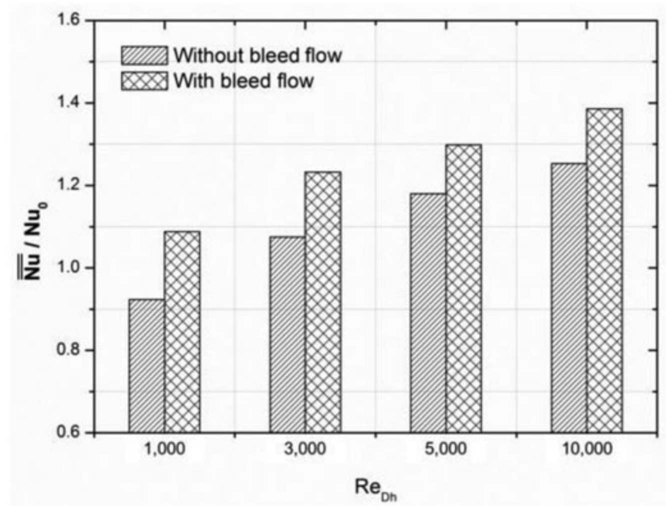

Figure 9 Normalized average Nusselt number.

Overall Performance

In Figure 9, the normalized average Nusselt number, $\overline{\overline{Nu}}/Nu_0$, is presented to quantitatively compare the average heat transfer performance. $\overline{\overline{Nu}}$ is the area-averaged Nusselt number calculated by Eq. (3). Nu_0 is the averaged Nusselt number on a smooth surface. This value is calculated for the

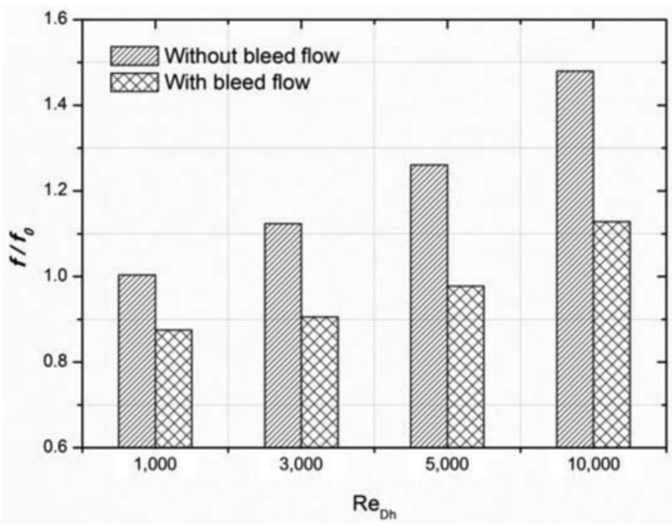

Figure 10 Normalized friction factor.

case respectively as a reference value for the evaluation of the normalized average Nusselt number. As with earlier studies, the heat transfer performance is enhanced as the Reynolds number increases. In the laminar flow regime ($Re_{Dh} = 1000$), the heat transfer performance of the dimple is lower than that of the smooth surface. This phenomenon is reported experimentally by Kwon et al. [8], and it is not recommended to use a dimpled surface in the laminar flow regime. It is clear that the heat transfer performance on a dimpled surface with bleed flow is superior to that on the dimpled surface without it. Heat transfer augmentation level in all cases of with bleed flow is higher by about 10–20% even in the laminar flow case.

In general, pressure loss should be considered together with heat transfer enhancement because it is directly related to the pumping power of thermal system. The friction factor is evaluated by Eq. (4) and presented in Figure 10. In ordinary heat exchangers, the pressure loss has to be increased as much as heat transfer performance is increased. Therefore, it looks unusual that the friction factor is lower than for the smooth surface with increased heat transfer performance in the case of the dimple with bleed flow. However, this can be accounted for by regarding the bleed hole as a secondary outlet of the channel. Even though only 0.5% of the mass flow rate of the main stream is effusing through the bleed hole, this amount of flow is large enough to reduce the recirculating flow that stagnates inside the dimple. As the size of the recirculating flow is diminished as much as the flow is effusing out, the effective cross-sectional area of the channel is increased and 99.5% of the main stream could more easily flow out via the channel. Though the friction factor is increasing as the Reynolds number increases, the friction factor in the case of the dimple with bleed flow is much lower than that in the case of the dimple without bleed flow. Consequently, the performance factor, PF, is presented in Figure 11. It is calculated by Eq. (5), which considers heat transfer performance and friction factor simultaneously to evaluate the overall performance of thermal system. Overall performance of the dimple is enhanced with bleed flow in the whole range of Reynolds numbers.

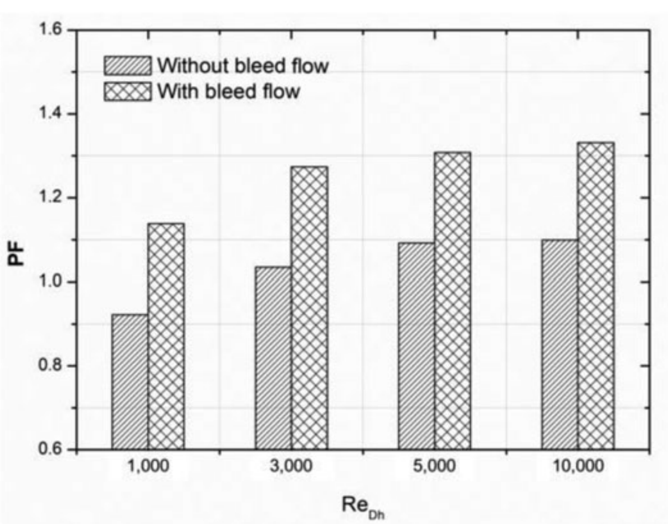

Figure 11 Performance factor.

Here is the limitation of the present study. Flow rate of bleed flow is fixed to a constant level in this simulation. But in a real situation, flow rate of bleed flow for film cooling in gas turbine engine is determined by the pressure difference between cooling air and hot gas. Pressure difference cannot be determined exactly in this simulation because the pressure of the cooling air and that of the hot gas are changed continuously as they flow and the bottom surface of the dimple shows a relatively lower pressure level than the periphery region. Therefore, correlation between pressure difference and bleed flow rate must be verified to implement this technique for operating a gas turbine engine, and further work would be required.

CONCLUSIONS

In the present study, the heat transfer enhancement method by combining dimple and bleed flow has been tested numerically at Reynolds numbers from 1,000 to 10,000. Two channels with dimple array are compared to identify effects of bleed flow on the heat transfer performance of dimple. The normalized Nusselt number and the friction factor are presented to evaluated heat transfer performance.

There is no significant heat transfer enhancement in the dimple cavity in the laminar flow regime. However in the turbulent flow regime, flow is turned to unsteady and distorted such that a transient asymmetric vortex appears inside the dimple cavity. Thus, flow disturbance enhances heat transfer performance on the dimple. Bleed flow in the dimple cavity affects the flow and heat transfer characteristic adjacent to the dimpled surface. Regardless of the flow condition, whether laminar or turbulent, the heat transfer rate is increased with bleed flow as the Reynolds number increases. As much as recirculating flow is effusing out through the bleed hole, the cooling air is drawn to the dimple cavity. Then the total flow rate into the dimple cavity is increased and the overall heat transfer performance is augmented. In addition, heat transfer at the bottom surface of the dimple cavity is also increased as the flow is accelerated in the vicinity of bleed hole. The heat transfer result shows good accord with the turbulent kinetic energy of fluid. In conclusion, it can be stated that local heat transfer in the dimple cavity can be improved with bleed holes for even 0.5% effusion of total mass flow.

NOMENCLATURE

d	dimple print diameter, mm
D_h	hydraulic diameter, mm
f	friction factor
f_0	friction factor for smooth channel
h	convective heat transfer coefficient, W/m^2-K
h_d	dimple depth, mm
H	height of channel, mm
k_{air}	thermal conductivity of air, W/m-K
L_1	length of channel, mm
L_2	length of investigation region
Nu	Nusselt number
Nu_0	averaged Nusselt number for smooth channel
$\overline{\overline{\mathrm{Nu}}}$	averaged Nusselt number in Eq. (3)
P	pitch of dimples, mm
ΔP	pressure difference, pa
PF	performance factor
Re	Reynolds number
T	temperature, K
U	averaged velocity at inlet, m/sec
W	width of channel, mm
x	coordinate in stream wise direction, mm
y	coordinate in height, mm
z	coordinate in span wise direction, mm

Greek Symbols

υ_{air}	dynamic viscosity of air, m^2/sec
ρ_{air}	density of air, kg/m^3

Subscripts

air	properties of air
d	depth
h	hydraulic

REFERENCES

[1] Ligrani, P. M., Oliveira, M. M., and Blaskovich, T., Comparison of Heat Transfer Augmentation Techniques, *AIAA Journal*, vol. 41, no. 3, pp. 337–362, 2003.

[2] Chyu, M. K., Yu, Y., and Ding, H., Heat Transfer Enhancement in Rectangular Channels With Concavities, *Enhanced Heat Transfer*, vol. 6, no. 6, pp. 429–439, 1999.

[3] Mahmood, G. I., Hill, M. L., Nelson, D. L., Ligrani, P. M., Moon, H. K., and Glezer, B., Local Heat Transfer and Flow Structure on and Above a Dimpled Surface in a Channel, *Journal of Turbomachinery*, vol. 123, no. 1, pp. 115–123, 2001.

[4] Burgess, N. K., and Ligrani, P. M., Effects of Dimple Depth on Channel Nusselt Numbers and Friction Factors, *Journal of Heat Transfer*, vol. 127, no. 8, pp. 839–847, 2005.

[5] Hwang, S. D., Kwon, H. G., and Cho, H. H., Heat Transfer With Dimple/Protrusion Arrays in a Rectangular Duct With a Low Reynolds Number Range, *International Journal of Heat and Fluid Flow*, vol. 29, pp. 916–926, 2008.

[6] Hwang, S. D., Kwon, H. G. and Cho, H. H., Local Heat Transfer and Thermal Performance on Periodically Dimple-Protrusion Patterned Walls for Compact Heat Exchangers, *Energy*, vol. 35, pp. 5357–5364, 2011.

[7] Kwon, H. G., *Heat/Mass transfer Enhancements on Dimpled Surfaces Using Vortex Controls*, Ph.D. thesis, Yonsei University, Korea, 2010.

[8] Kwon, H. G., Hwang, S. D. and Cho, H. H., Measurement of Local Heat/Mass Transfer Coefficients on a Dimple Using Naphthalene Sublimation, *International Journal of Heat and Mass Transfer*, vol. 54, no. 5–6, pp. 1071–1080, 2011.

[9] Isaev, S. A., and Leont'ev, A. I., Numerical Simulation of Vortex Enhancement of Heat Transfer Under Conditions of Turbulent Flow Past a Spherical Dimple on the Wall of a Narrow Channel, *High Temperature*, vol. 41, no. 5, pp. 665–679, 2003.

[10] Kim, K. M., Kim, S. I., Jeon, Y. H., Lee, D. H., and Cho, H. H., Detailed Heat/Mass Transfer Distributions in a Rotating Smooth Channel With Bleed, *Journal of Heat Transfer*, vol. 129, pp. 1538–1545, 2007.

[11] Taslim, M. E., Li, T., and Spring, S. D., Experimental Study of the Effects of Bleed Holes on Heat Transfer and Pressure Drop in Trapezoidal Passages With Tapered Turbulators, *Journal of Turbomachinary*, vol. 117, pp. 281–289, 1995.

[12] Shen, J. R., Wang, Z., Ireland, P. T., Jones, T. V., and Byerley, A. R., Heat Transfer Enhancement Within a Turbine Blade Cooling Passage Using Ribs and Combinations of Ribs With Film Cooling Holes, *Journal of Turbomachinary*, vol. 118, pp. 428–434, 1996.

[13] Thurman, D., and Poinastte, P., Experimental Heat Transfer and Bulk Air Temperature Measurements for a Multipass Internal Cooling Model With Ribs and Bleed, *Journal of Turbomachinary*, vol. 123, pp. 90–96. 2001.

[14] Jeon, Y. H., Park, S. H., Kim, K. M., Lee, D. H., and Cho, H. H., Effects of Bleed Flow on Heat/Mass Transfer in a Rotating Rib-Roughened Channel, *Journal of Turbomachinary*, vol. 129, no. 3, pp. 636–642, 2007.

[15] Gortyshov, Y., and I. Popov, The Scientific Basis of Calculations of Highly Efficient Compact Heat-Transfer Apparatuses With Judicious Heat-Transfer Intensifiers, *Thermal Engineering*, vol. 53, no. 4, pp. 249–261, 2006.

[16] Park, J., Desam, P. R., and Ligrani, P. M., Numerical Predictions of Flows Structure Above a Dimpled Surface in a Channel, *Numerical Heat Transfer, Part A: Applications*, vol. 45, no. 1, pp. 1–20, 2004.

Heeyoon Chung received his B.S. in mechanical engineering from Yonsei University in 2011 and is currently a graduate student working on a combined master's and doctorate program at the Department of Mechanical Engineering of the same university. His research interest is heat transfer in high-temperature gas turbines. It specifically includes thermal design for prediction and prevention of thermally induced stresses that can cause cracks on turbine components.

Kyung Min Kim is a senior researcher in the CHP and DH technology team at Korea District Heating Corporation (KDHC). He received his Ph.D. in mechanical engineering from Yonsei University, Seoul, Korea, in 2008. He has been working at KDHC in the field of heat transfer design of thermal systems since August 2011. His research activities and interests are in the area of thermal design, management, and optimization in energy and power applications.

Hyun Goo Kwon is principal researcher of Technovalue, Seoul, Korea. He received his Ph.D. in mechanical engineering from Yonsei University in 2010. He focused his research interest on internal channel flow with corrugated surfaces such as dimple and protrusion during the period of his doctorate course. His current major research interest is thermal management in development of the continuous Czochalski process to produce single-crystal silicon ingots.

Sanghoon Lee received his B.S. degree in mechanical engineering from Yonsei University in 2003. Since entering the graduate college at Yonsei in 2005, he has studied the flooding phenomenon, water management, and performance enhancement of PEMFCs as a Ph.D. candidate. He has also been involved in analyzing flow structure on complicated surfaces with dimples and protrusions.

Beom Seok Kim is a postdoctoral researcher at the Heat Transfer Laboratory in Yonsei University, South Korea. He received his Ph.D. (mechanical engineering) in 2011 from Yonsei University, South Korea. His main research topics include micro-/nanoscale thermal-hydraulic experiments and analysis on heat transfer and optimization based on the response surface method.

Hyung Hee Cho received the Ph.D. degree in mechanical engineering from the University of Minnesota, Minneapolis, in 1992. Since 1995, he has been with the Department of Mechanical Engineering, Yonsei University, Seoul, Korea, where he is currently a full professor in the School of Mechanical Engineering. He is currently an associate editor of the *International Journal of Fluid Machinery and Systems*, and an editorial board member of *Advances in Mechanical Engineering* and the JP *Journal of Heat and Mass Transfer*. His research interests include thermal management and cooling of high temperature devices. He is a fellow of the American Society of Mechanical Engineers, a scientific council member of the International Centre for Heat and Mass Transfer, and an associate member of the Korea Academy of Science and Technology.